Transversality Across Two Distinct Quantum Codes and Its Application to Quantum Repeaters

Mahdi Bayanifar[1], Alexei Ashikhmin[2], Dawei Jiao[1], Olav Tirkkonen[1]

[1]*Department of Communications and Networking, Aalto University, Finland*
[2]*Nokia Bell Labs, Murray Hill, New Jersey, USA*
Email: {mahdi.bayanifar, dawei.jiao, olav.tirkkonen}@aalto.fi
alexei.ashikhmin@nokia-bell-labs.com

***Abstract*—In this work, we generalize the concept of transversality in quantum error-correcting codes. Unlike conventional methods, we study transversal logical two-qubit gates between two different codes. We consider an application of this concept for quantum networks which consist of multiple intermediate stations equipped with quantum repeaters (QRs). The stations may experience different error models. For instance, in one station, a particular Pauli error may dominate, whereas in its neighboring stations, other types of Pauli errors are more likely. The standard approach of using the same CSS code $\mathcal{Q}$ in different stations does not allow for simultaneously adaptating $\mathcal{Q}$ to be optimized to the errors prevailing in various stations. Considering this fact, we suggest using different CSS codes in each station. In this work, we analyze CNOT and CZ transversality for pairs of CSS codes and provide a complete characterization. We formulate necessary and sufficient conditions for a pair of CSS codes to be CNOT and CZ transversal. In comparison to the conventional approach of having the same CSS code, we show that these conditions are less restrictive.**

***Index Terms*—Transversality, CSS codes, CNOT gate, CZ gate, Quantum repeaters.**

I. Introduction

In order to achieve high accuracy in quantum computations, the gates should be implemented in a fault-tolerant manner. The transversal gate implementation is a natural way to ensure fault-tolerant gates, wherein the gates do not entangle different physical qubit subsystems within a code, and errors will not accumulate [1].

The conventional way of using quantum error correction code (QECC) is to have the same code for each code block and conduct error correction procedure [2]. However, in some scenarios, different system suffer from different biased errors, and using different QECCs will provide better performance in comparison to using the same QECCs. One particular example is the quantum repeaters (QRs) which are widely have been used in quantum communication realm as they can extent the distance and reliability of information transmission [3].

We consider 2nd generation of QRs which currently are most likely to be implemented in near-term quantum devices [4]. In the 2nd generation QRs, QECCs are used in each station to correct the transmission and local operation errors. The communication protocol is based on logical entanglement between different stations, and in order to avoid error propagation the protocol should be fault-tolerant, which requires that QECCs used in neighboring stations were CNOT-transversal [5].

In [3] error models appearing in the communication protocol of the 2nd generation QRs have been analyzed, and showed that the errors occurring in neighboring stations are biased and correlated. For instance, the Pauli $\mathbf{X}$ error could be more likely in one station and $\mathbf{Z}$ errors more likely in the neighboring station. Authors introduced a CSS code based structure called mirrored structure to overcome the biased and correlated errors. The reason for these biased and correlated errors arises from the Bell state purification and remote CNOT procedures [6]. Based on the above error model, it has been proposed to design and optimize QECCs specifically [3]. Intuitively, they proposed to use different CSS codes in nearby stations, one with larger resistance to $\mathbf{X}$ errors, and another with larger resistance to $\mathbf{Z}$ errors. However, such CSS codes may be non transversal, which will lead to a non fault-tolerant communication protocol. This motivates us to study conditions on code pairs be transversal.

Motivated by the above reasons, in this paper we study the non-local CNOT and CZ-transversality of pairs of CSS codes used for establishing neighboring entanglement. Note that this differs from the logical CNOT gates used in the entanglement swapping procedure, which consist of only local operations.

In our studies, we first provide conditions on the non-local CNOT-transversality between CSS codes used in nearby stations. We observe that in contrast to the well known fact that for having a CNOT transversal gate, one needs to have the same code in the station, less restrictive conditions are needed. Although using transversal CNOT gate to achieve non-local logical CNOT gate is common, another alternative is using local logical Hadamard and non-local logical CZ gate. Then, we investigate the transversality of the non-local CZ gates and find sufficient conditions for achieving the CZ-transversality. We show that for achieving the transversality, one needs to select the mapping properly and otherwise the transversality may not hold. As an example of transversal CZ-gate, we investigate the mirrored structure. This structure could get better result under the 2nd generation QRs error model than using the same code in every station. We show that any mirrored structure could achieve sufficient condition of non-local CZ-transversality. Furthermore, through some examples, we show that for achieving the transversality, one needs to select the mapping properly and otherwise the transversality may not hold. Finally using simulation results, we show that the optimal performance region of the CNOT and CSS transversal codes are different and depending on the error model either using transversal CNOT or CZ gate could achieve better performance.

Note that our approach establishes the transversality between different codes and may provide a new path to the fault-tolerant universal quantum computation beyond the 2nd generation of QRs. It is worth noting that the transversality between two different codes is not only used for QRs system, but also can be applied in quantum computation, like distributed quantum computation, or other realms.

The paper is organized as follows: We review basic definitions of CSS codes in II. In Section III we consider communication protocol and error models happened before the entanglement swapping procedure. Next, we establish conditions on code pairs to be CNOT and CZ-transversal IV. Section V provides simulations results and finally, Section VI concludes the paper.

II. Qubits, Quantum Operations, and CSS codes

In this section, we recall the main definitions of quantum CSS codes. More details on this can be found, e.g., in [7].

Let $\mathbf{v} = (v_1, ..., v_n) \in \mathbb{F}_2^n$ and $|0\rangle = (1,0)^T$, $|1\rangle = (0,1)^T \in \mathbb{C}^2$. Then the quantum states $|\mathbf{v}\rangle = |v_1\rangle \otimes \dots |v_n\rangle$ form the computational basis of $\mathbb{C}^{2^n}$, and any pure state $|\psi\rangle \in \mathbb{C}^{2^n}$ of n qubits can be written in the form

$$|\boldsymbol{\psi}\rangle = \sum_{\mathbf{v}\in\mathbb{F}_2^n} \alpha_{\mathbf{v}} |\mathbf{v}\rangle, \qquad (1)$$
$$\text{where } \sum_{\mathbf{v}\in\mathbb{F}_2^n} |\alpha_v|^2 = 1.$$

The CNOT gate between a control qubit in a pure state $|\psi\rangle$ and target qubit in $|\xi\rangle$ corresponds to the unitary transformation $\mathbf{U}_{CNOT}(|\psi\rangle \otimes |\xi\rangle)$, where

$$\mathbf{U}_{CNOT} = \begin{bmatrix} 1 & 0 & 0 & 0 \\ 0 & 1 & 0 & 0 \\ 0 & 0 & 0 & 1 \\ 0 & 0 & 1 & 0 \end{bmatrix}.$$

For $a, b \in \mathbb{F}_2$ we have $\mathbf{U}_{CNOT}(|a\rangle \otimes |b\rangle) = |a\rangle \otimes |a+b\rangle$. Denote by $\mathbf{U}_{CNOT,i,i+n} \in \mathbb{C}^{2^{2n}}$ the gate that conducts the CNOT for qubits i and $n+i$ and leave other qubits untouched. Assume that we have two sets of n qubits in pure states

$$|\boldsymbol{\psi}\rangle = \sum_{\mathbf{v}\in\mathbb{F}_2^n} \alpha_{\mathbf{v}} |\mathbf{v}\rangle, \text{ and } |\boldsymbol{\xi}\rangle = \sum_{\mathbf{w}\in\mathbb{F}_2^n} \beta_{\mathbf{w}} |\mathbf{w}\rangle,$$

and denote by $CNOT$ the operator that conducts CNOT gates for all the qubit pairs $(i, n+i), i = 1, \dots, n$. It is not difficult to see that

$$\begin{aligned} & CNOT(|\boldsymbol{\psi}\rangle \otimes |\boldsymbol{\xi}\rangle) \\ &= (\mathbf{U}_{CNOT,1,n+1}\mathbf{U}_{CNOT,2,n+2} \dots \mathbf{U}_{CNOT,n,2n}) (|\boldsymbol{\psi}\rangle \otimes |\boldsymbol{\xi}\rangle) \\ &= \sum_{\mathbf{v}\in\mathbb{F}_2^n} \sum_{\mathbf{w}\in\mathbb{F}_2^n} \alpha_{\mathbf{v}}\beta_{\mathbf{w}} (|\mathbf{v}\rangle \otimes |\mathbf{v}+\mathbf{w}\rangle). \end{aligned} \qquad (2)$$

Similar definitions can be made for quantum mixed states, but we omit those details. Recall that Control-Z (CZ) gate is defined by $\mathbf{U}_{CZ} = \text{diag}(1,1,1,-1)$. We denote by CZ the operator that applies CZ gates to all the qubit pairs $(i, n+i), i = 1, \dots, n$. It is again not difficult to see that

$$CZ(|\boldsymbol{\psi}\rangle \otimes |\boldsymbol{\xi}\rangle) = \sum_{\mathbf{v}\in\mathbb{F}_2^n} \sum_{\mathbf{w}\in\mathbb{F}_2^n} (-1)^{\mathbf{v}\mathbf{w}^T} \alpha_{\mathbf{v}}\beta_{\mathbf{w}} (|\mathbf{v}\rangle \otimes |\mathbf{w}\rangle). \qquad (3)$$

The widely used completely depolarizing error model is described by the Pauli matrices:

$$\mathbf{X} \triangleq \begin{bmatrix} 0 & 1 \\ 1 & 0 \end{bmatrix}, \ \mathbf{Z} \triangleq \begin{bmatrix} 1 & 0 \\ 0 & -1 \end{bmatrix} \ \mathbf{Y} \triangleq \begin{bmatrix} 0 & -i \\ i & 0 \end{bmatrix}, \qquad (4)$$

where $i \triangleq \sqrt{-1}$. For $\mathbf{a}, \ \mathbf{b} \in \mathbb{F}_2^n$ we define operator

$$\mathbf{D}(\mathbf{a}, \mathbf{b}) = \mathbf{X}^{a_1}\mathbf{Z}^{b_1} \otimes ... \otimes \mathbf{X}^{a_n}\mathbf{Z}^{b_n}.$$

Let $\mathcal{C}_1$ and $\mathcal{C}_2$ be two classical linear codes with parameters $[n, k_1, d_1]$ and $[n, k_2, d_2]$, respectively. By $\mathcal{C}_1^\perp$ and $\mathcal{C}_2^\perp$ we denote their dual codes of dimensions $k_1^\perp$ and $k_2^\perp$ respectively. Let also the property $\mathcal{C}_2^\perp \subset \mathcal{C}_1$ hold. Then $\mathcal{C}_1$ and $\mathcal{C}_2$ define an $[[n,k,d]], k = k_1 + k_2 - n, d = \min(d_1, d_2)$, quantum CSS $(\mathcal{C}_1, \mathcal{C}_2)$ code, which is a linear subspace of dimension 2^k in $\mathbb{C}^{2^n}$. Let us assume that there is a linear bijection between vectors $\boldsymbol{\psi} \in \mathbb{F}_2^k$ and representatives $\mathbf{x} \in \mathcal{C}_1$ of cosets of $\mathcal{C}_2^\perp$ in the quotient group $\mathcal{C}_1/\mathcal{C}_2^\perp$. Then CSS $(\mathcal{C}_1, \mathcal{C}_2)$ poses the orthogonal basis

$$|\boldsymbol{\psi}\rangle_L = \frac{1}{\sqrt{|\mathcal{C}_2^\perp|}} \sum_{\mathbf{y}\in\mathcal{C}_2^\perp} |\mathbf{x}+\mathbf{y}\rangle. \qquad (5)$$

It is worth noting that the CSS codes are special case of the stabilizer codes. This means that for any $[[n,k,d]]$ CSS code Q, we can find a commutative group $\mathcal{S}, |\mathcal{S}| = 2^{n-k}$, composed by operators $\gamma_{\mathbf{a},\mathbf{b}} D(\mathbf{a},\mathbf{b})$ where $\gamma_{\mathbf{a},\mathbf{b}}$ is either 1 or -1. For any $\gamma_{\mathbf{a},\mathbf{b}} D(\mathbf{a},\mathbf{b}) \in \mathcal{S}$, we have

$$\gamma_{\mathbf{a},\mathbf{b}} D(\mathbf{a},\mathbf{b}) |\boldsymbol{\psi}\rangle = |\boldsymbol{\psi}\rangle, \text{ for any } |\boldsymbol{\psi}\rangle \in Q.$$

The vectors $(\mathbf{a}, \mathbf{b})$, defining the operators $\gamma_{\mathbf{a},\mathbf{b}} D(\mathbf{a},\mathbf{b}) \in \mathcal{S}$, form the linear code with the generator matrix

$$\mathbf{G}^{\mathcal{Q}} = \left[\begin{array}{c:c} \mathbf{G}_2^\perp & \mathbf{0} \\ \hdashline \mathbf{0} & \mathbf{G}_1^\perp \end{array}\right].$$

III. Quantum Network with Quantum Codes Matched to Error Model

A typical quantum network link is shown in Fig.1. The intermediate stations contain QRs and possibly other hardware. In this work we assume that QRs of the 2nd generation are used. The 2nd generation QRs use quantum codes to suppress the procedure errors, as we discuss it below. Using quantum codes is efficient in terms of achieving high fidelity and makes the requirements on the quantum hardware and its control relevantly low and therefore more achievable with near-term quantum devices [4]. In this paper, following work from [3], we assume CSS codes $[[n,k,d]]$, k logical qubits encoded into n physical qubits with code distance d.

Next, as we argue below, type of errors in stations along a quantum link can vary significantly. So, we suggest to use different CSS codes in different stations, and match the codes to particular error models of the stations. We assume that the neighboring stations A and B use $CSS(\mathcal{C}_1,\mathcal{C}_2)$, and $CSS(\mathcal{C}_3,\mathcal{C}_4)$ codes respectively, where $\mathcal{C}_3$ and $\mathcal{C}_4$, $\mathcal{C}_4^\perp \subset \mathcal{C}_3$, are classical codes with parameters $[n,k_3,d_3]$ and $[n,k_4,d_4]$ respectively, such that $n-k = k_3+k_4 = k_1+k_2$. By $\mathcal{C}_3^\perp$ and $\mathcal{C}_4^\perp$ we denote their dual codes of dimensions $k_3^\perp$ and $k_4^\perp$ respectively. We assume that the following protocol is conducted between neighboring stations.

Neighboring Stations Entanglement Swapping

1) Stations A and B prepare their k logical qubits $q_1^A,\dots,q_k^A$ and $q_1^B,\dots,q_k^B$ in the states $q_j^A = |+\rangle_L = |0\rangle_L + |1\rangle_L$, and $q_j^B = |0\rangle_L$, $j=1,\dots,k$, respectively. Further they encode the logical qubits into n physical qubits $p_1^A,\dots,p_n^A$ and $p_1^B,\dots,p_n^B$ with $CSS(\mathcal{C}_1,\mathcal{C}_2)$ and $CSS(\mathcal{C}_3,\mathcal{C}_4)$ codes respectively.
2) Station A generates $N > n$ Bell pairs qubits, e.g, photons, in $|00\rangle + |11\rangle$ state, and sends the second qubit of each pair to station B via a classical link, e.g., optic fiber.
3) Stations A and B conduct K level purification procedure for the N Bell pairs, see [8], and obtain n shared (noisy) Bell pairs $c_1^A,c_1^B;\dots;c_n^A,c_n^B$.
4) Stations A and B conduct local operations shown in Fig.2 using their qubits $p_1^A,\dots,p_n^A$ (green dots) and $c_1^A,\dots,c_n^A$ (gray dots) and $p_1^B,\dots,p_n^B$, $c_1^B,\dots,c_n^B$ respectively, with $\mathbf{U} = \mathbf{U}_{CNOT}$ from green to gray qubit in Station A and from gray to green qubit in Station B. By doing this Stations A and B effectively conduct remote CNOT operations between p_j^A and p_j^B, $j=1,\dots,n$.
5) Stations A and B correct errors in their physical qubits using decoders of $CSS(\mathcal{C}_1,\mathcal{C}_2)$ and $CSS(\mathcal{C}_3,\mathcal{C}_4)$, respectively.

It is important to note that under the assumption that codes $CSS(\mathcal{C}_1,\mathcal{C}_2)$ and $CSS(\mathcal{C}_3,\mathcal{C}_4)$ are CNOT-transversal (see a formal definition in the next Section), at Step 5 the physical qubits at Stations A and B are turned into the encoded states of these codes corresponding to logical qubits $|q_j^A\ q_j^B\rangle = |00\rangle + |11\rangle$, $j=1,\dots,k$. Therefore conducting the above protocol for the Stations along the network link, and further applying entanglement swapping one achieves long-distance entanglement between k pairs of the logical qubits in the terminal Stations of the network link [9], which requires less resources for achieving a target fidelity in comparison to a direct use of the Bell state purification procedure [10].

The purified Bell states at Step 3 are still noisy and that noise propagates to physical qubits $p_1^A,\dots,p_n^A,p_1^B,\dots,p_n^B$ through the gate of the circuit shown in Fig.2. This results in a complex error model for the physical qubits. One such model was introduced and analysed recently in [3]. Let ρ denote the error-free joint density matrix of physical qubits p_j^A and p_j^B for some fixed j after conducting the remote CNOT. Then, according to the error model from [3], the physical qubits will have the density matrix

$$\mathcal{N}(\boldsymbol{\rho}) = \left(1-\sum_{i=1}^{3} f_i\right)[\mathbf{I}_A\mathbf{I}_B](\boldsymbol{\rho}) \ + \ f_1[\mathbf{Z}_A\mathbf{I}_B](\boldsymbol{\rho}) + f_2[\mathbf{I}_A\mathbf{X}_B](\boldsymbol{\rho}) + f_3[\mathbf{Z}_A\mathbf{X}_B](\boldsymbol{\rho}),\ 0 \le f_1, f_2.f_3 \le 1, \tag{6}$$

where $\mathbf{P}_A$ and $\mathbf{P}_B$ denote the operation $\mathbf{P}$ in Stations A and B, respectively; and $[\mathbf{U}_1\mathbf{U}_2](\boldsymbol{\rho})$ denotes $(\mathbf{U}_1\otimes\mathbf{U}_2)\boldsymbol{\rho}(\mathbf{U}_2^\dagger\otimes\mathbf{U}_1^\dagger)$. Note that f_1 is the probability of errors $\mathbf{Z}$ in Station A and the absence of errors in Station B, while f_2 is the probability of $\mathbf{X}$ errors in Station B, and f_3 is the probability of correlated errors. It was observed in [3] that typically one type of errors dominates. For example, we may have that $f_1 > f_2 >> f_3$. So, it is desirable to use different CSS codes, say Q_1 and Q_2 in Stations A and B, as it is shown in Fig.1. By adjusting these codes to error models of Stations A and B, we can significantly improve the fidelity, reduce time cost, and so on. However, it is important to remember that we cannot use arbitrary CSS codes since the codes should be CNOT-transversal.

In the next Sections we study the main principles of construction of CNOT-transversal CSS codes. In [3] it was shown that if CZ-transversal codes are used in Stations A and B, then the Local Swapping Protocol can be modified by logical Hadamard gates, using either magic states or local operations [11]. Thus, one can still implement the needed non-local CNOT operation with rather low overhead. For this reason, we also study the construction of CZ-transversal codes.

IV. Transversality of CSS Codes

First we would like to recall the well known fact that if the same CSS code is used in Stations A and B then we have CNOT-transversality granted and therefore can implement Local Swapping Protocol. However, as we explained above, due to asymmetry of errors it would more beneficial to use different CSS codes in neighboring Stations.

Let us assume that use two CSS$(\mathcal{C}_1,\mathcal{C}_2)$ and CSS$(\mathcal{C}_3,\mathcal{C}_4)$ codes in stations A and B, respectively. Our objective is to find suitable conditions that would guarantee CNOT and/or CZ-transversality of these codes. Let $\mathbf{G}_2^\perp$ and $\mathbf{G}_4^\perp$ be generator

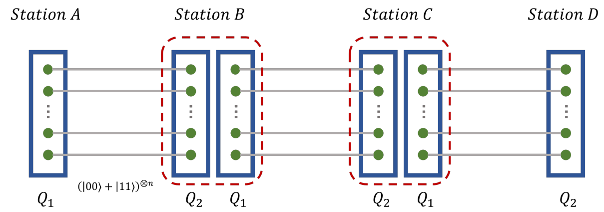

Fig. 1. Q_1 and Q_2 are different CSS codes with higher capability for correcting Pauli Z and X errors. These codes are designed to provide CNOT (or CZ) transversality between Stations A and B, corresponding to the bias created by the non-local CNOT protocol. Using the same Q_1-code at Station B enables local transversal CNOT within the station. End-to-end entanglement can thus be created with transversal operations using these two codes. Alternatively, the same CSS Q1-code can be used at Station B that enables implementation of transversal CNOT since any CSS code is CNOT-transversal.

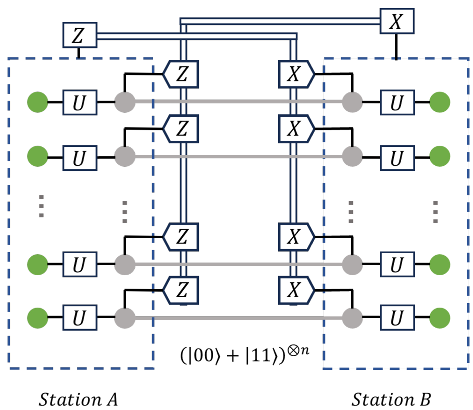

Fig. 2. The transversal non-local gate schematic: Unitary operator $\mathbf{U}$ can be selected as CNOT or CZ gate in order to achieve transversal non-local CNOT (green qubit as control) or CZ gate. After implementing $\mathbf{U}$ operator, these Bell states (gray dots), are measured in Pauli Z and X bases. According to the outcome, the feedback Pauli X and Z operation will be applied on physical qubits (green dots) in each station.

matrices of $\mathcal{C}_2^\perp$ and $\mathcal{C}_4^\perp$, respectively. Then, the generator matrices of $\mathcal{C}_1$ and $\mathcal{C}_3$ can be written in the following form

$$\mathbf{G}_1 = \begin{bmatrix} \mathbf{G}_2^\perp \\ \mathbf{A} \end{bmatrix}, \qquad \mathbf{G}_3 = \begin{bmatrix} \mathbf{G}_4^\perp \\ \mathbf{B} \end{bmatrix}, \tag{7}$$

where $\mathbf{A}$ and $\mathbf{B}$ are $k \times n$ binary matrices of rank k.

We will use $\mathbf{A}$ and $\mathbf{B}$ for defining the linear bijections between vectors $\boldsymbol{\psi}^A, \boldsymbol{\psi}^B \in \mathbb{F}_2^k$ and representatives $\mathbf{x}^A \in \mathcal{C}_1$ and $\mathbf{x}^B \in \mathcal{C}_3$ of cosets in the quotient groups $\mathcal{C}_1/\mathcal{C}_2^\perp$ and $\mathcal{C}_3/\mathcal{C}_4^\perp$. With these bijections the code vectors of CSS$(\mathcal{C}_1, \mathcal{C}_2)$ and CSS$(\mathcal{C}_3, \mathcal{C}_4)$ corresponding to logical qubits in the states $|\boldsymbol{\psi}^A\rangle$ and $|\boldsymbol{\psi}^B\rangle$ are

$$|\boldsymbol{\psi}^A\rangle_L = \frac{1}{\sqrt{|C_2^\perp|}} \sum_{\mathbf{y}\in C_2^\perp} |\mathbf{x}^A + \mathbf{y}\rangle \tag{8}$$

$$|\boldsymbol{\psi}^B\rangle_L = \frac{1}{\sqrt{|C_4^\perp|}} \sum_{\mathbf{z}\in C_4^\perp} |\mathbf{x}^B + \mathbf{z}\rangle, \tag{9}$$

where $\mathbf{x}^A = \boldsymbol{\psi}^A\mathbf{A}$ and $\mathbf{x}^B = \boldsymbol{\psi}^B\mathbf{B}$ which we call them mapping matrices.

Theorem 1. *Codes CSS$(\mathcal{C}_1, \mathcal{C}_2)$ and CSS$(\mathcal{C}_3, \mathcal{C}_4)$ are CNOT-transversal, with CSS$(\mathcal{C}_1, \mathcal{C}_2)$ being the control and CSS$(\mathcal{C}_3, \mathcal{C}_4)$ the target code, iff*

$$\mathcal{C}_2^\perp \subseteq \mathcal{C}_4^\perp \tag{10}$$

$$\mathcal{C}_1/\mathcal{C}_2^\perp \cong \mathcal{C}_3/\mathcal{C}_4^\perp \tag{11}$$

Proof. For showing the transversality, we need to show that applying CNOT gates to k pairs of logical qubits in the states $|\boldsymbol{\psi}^A\rangle$ and $|\boldsymbol{\psi}^B\rangle$, and then encoding the results into code vectors of CSS$(\mathcal{C}_1, \mathcal{C}_2)$ and CSS$(\mathcal{C}_3, \mathcal{C}_4)$ gives the same result as applying CNOT operations to n pairs of physical qubits in states $|\boldsymbol{\psi}^A\rangle_L$ and $|\boldsymbol{\psi}^B\rangle_L$ defined in (8) and (9).

If we first apply CNOT gates to logical qubits and then conduct encoding into code vectors of CSS$(\mathcal{C}_1, \mathcal{C}_2)$ and CSS$(\mathcal{C}_3, \mathcal{C}_4)$. According to (2), we will get the result

$$|\boldsymbol{\psi}^A\rangle_L \otimes |\boldsymbol{\psi}^A \oplus \boldsymbol{\psi}^B\rangle_L, \tag{12}$$

where using definition in (8), and according to (5) and (7),

$$|\boldsymbol{\psi}^A \oplus \boldsymbol{\psi}^B\rangle_L = \frac{1}{\sqrt{|\mathcal{C}_4^\perp|}} \sum_{\mathbf{y}\in C_4^\perp} |\left(\boldsymbol{\psi}^A + \boldsymbol{\psi}^B\right)\mathbf{B} + \mathbf{y}\rangle. \tag{13}$$

Next, if we apply CNOT gates to the n pairs of physical qubits encoded into states defined in (8) and (9) then, according to (2), we get the state

$$\begin{aligned} &\text{CNOT}(|\boldsymbol{\psi}^A\rangle_L \otimes |\boldsymbol{\psi}^B\rangle_L) \\ &= \frac{1}{\sqrt{|\mathcal{C}_2^\perp|\,|\mathcal{C}_4^\perp|}} \sum_{\mathbf{y}\in\mathcal{C}_2^\perp, \mathbf{z}\in\mathcal{C}_4^\perp} |\mathbf{x}^A + \mathbf{y}\rangle \otimes |\mathbf{x}^A + \mathbf{x}^B + \mathbf{y} + \mathbf{z}\rangle \\ &\overset{(a)}{=} \frac{1}{\sqrt{|\mathcal{C}_2^\perp|\,|\mathcal{C}_4^\perp|}} \sum_{\mathbf{y}\in\mathcal{C}_2^\perp, \mathbf{z}'\in\mathcal{C}_4^\perp} |\mathbf{x}^A + \mathbf{y}\rangle \otimes |\mathbf{x}^A + \mathbf{x}^B + \mathbf{z}'\rangle, \end{aligned} \tag{14}$$

where (a) is true iff $\mathcal{C}_2^\perp \subseteq \mathcal{C}_4^\perp$ or equivalently $\mathcal{C}_4 \subseteq \mathcal{C}_2$.

For achieving the transversality we need that (13) be equal to (14) for any $\boldsymbol{\psi}^A$ and $\boldsymbol{\psi}^B$. This is possible if and only if $\mathbf{A} = \mathbf{B}$, and this means that $\mathcal{C}_1/\mathcal{C}_2^\perp \cong \mathcal{C}_3/\mathcal{C}_4^\perp$. Note that the cosets in $\mathcal{C}_1/\mathcal{C}_2^\perp$ and $\mathcal{C}_3/\mathcal{C}_4^\perp$ may contain different number of vectors, since $\mathcal{C}_2^\perp$ can be smaller than $\mathcal{C}_4^\perp$, but the quotient groups are still isomorphic if $\mathbf{A} = \mathbf{B}$. □

Note that considering (7) and CNOT-transversality constraints given in (10) and (11), we can rewrite the generators of $\mathcal{C}_1$ and $\mathcal{C}_2$ as follows

$$\mathbf{G}_1 = \begin{bmatrix} \mathbf{G}_2^\perp \\ \mathbf{A} \end{bmatrix}, \qquad \mathbf{G}_3 = \begin{bmatrix} \mathbf{G}_2^\perp \\ \mathbf{D} \\ \mathbf{A} \end{bmatrix}, \tag{15}$$

where $\mathbf{D}$ is a $(k_4^\perp - k_2^\perp) \times n$ matrix of the rank $k_4^\perp - k_2^\perp$, which serves as a generator of $\mathcal{C}_4^\perp/\mathcal{C}_2^\perp$. Note that this structure implies that $\mathcal{C}_1 \subset \mathcal{C}_3$ and may prompt one to conclude that it is sufficient to have $\mathcal{C}_1 \subset \mathcal{C}_3$ for achieving CNOT-transversality. However, this is not correct. For example we can consider the case that $\mathcal{C}_1 = \mathcal{C}_4^\perp \subset \mathcal{C}_3$, i.e.,

$$\mathbf{G}_1 = \begin{bmatrix} \mathbf{G}_2^\perp \\ \mathbf{A} \end{bmatrix}, \qquad \mathbf{G}_3 = \begin{bmatrix} \mathbf{G}_2^\perp \\ \mathbf{A} \\ \mathbf{D} \end{bmatrix}.$$

In this example $\mathcal{C}_1 \subset \mathcal{C}_3$, however this configuration does not satisfy the property given in (11). Below we give an example of two different CSS codes that CNOT-transversal.

Example 1. *The following CSS codes of length $n = 7$ with $k_1 = 4$, $k_2 = 5$, and $k_3 = 5$, $k_4 = 4$ respectively and generator matrices*

$$\mathbf{G}_1 = \begin{bmatrix} \mathbf{G}_2^{\perp} \\ \mathbf{A} \end{bmatrix} = \begin{bmatrix} 1 & 1 & 0 & 0 & 0 & 0 & 0 \\ 0 & 1 & 0 & 1 & 1 & 1 & 1 \\ \hdashline 0 & 0 & 1 & 1 & 0 & 1 & 1 \\ 1 & 0 & 1 & 1 & 1 & 0 & 0 \end{bmatrix}$$

$$\mathbf{G}_3 = \begin{bmatrix} \mathbf{G}_2^{\perp} \\ \mathbf{D} \\ \mathbf{A} \end{bmatrix} = \begin{bmatrix} 1 & 1 & 0 & 0 & 0 & 0 & 0 \\ 0 & 1 & 0 & 1 & 1 & 1 & 1 \\ \hdashline 0 & 1 & 1 & 1 & 0 & 1 & 0 \\ \hdashline 0 & 0 & 1 & 1 & 0 & 1 & 1 \\ 1 & 0 & 1 & 1 & 1 & 0 & 0 \end{bmatrix},$$

satisfy the conditions of Theorem 1. Thus, these CSS codes are transversal. This example shows that one can find codes with different parameters and structures to fit a particular error model in neighboring Stations of a quantum network. For instance, one code can be better protected against X errors and another code against Z errors. Moreover, nonidentical code allows correcting drastically better correlated errors in the neighboring stations compared to using an identical codes in both stations. Detailed research on this will be presented in future works.

It is common to use transversal CNOT gate to achieve non-local logical CNOT gate. Also, using a local logical Hadamard and a non-local logical CZ gate, we can achieve a non-local logical CNOT gate. Let us now consider the CZ transversality. In the following theorem, we define the conditions for CSS codes to be CZ-transversal.

Theorem 2. *Codes CSS$(\mathcal{C}_1, \mathcal{C}_2)$ and CSS$(\mathcal{C}_3, \mathcal{C}_4)$ are CZ transversal iff*

$$\mathbf{A}\mathbf{B}^T = \mathbf{I}\,, \tag{16}$$

and for all $\mathbf{y} \in \mathcal{C}_2^{\perp}$, $\mathbf{z} \in \mathcal{C}_4^{\perp}$ and $\boldsymbol{\psi}^A, \boldsymbol{\psi}^B \in \mathbb{F}_2^k$ we have

$$\mathbf{x}^A \mathbf{z}^T + \mathbf{y}\left(\mathbf{x}^B + \mathbf{z}\right)^T = 0\,, \tag{17}$$

where

$$\begin{aligned} \mathbf{x}^A &= \boldsymbol{\psi}^A \mathbf{A}, \\ \mathbf{x}^B &= \boldsymbol{\psi}^B \mathbf{B}\,. \end{aligned}$$

Proof. According to (3), if we apply CZ operations to the k pairs of logical qubits in the states $|\boldsymbol{\psi}^A\rangle$ and $|\boldsymbol{\psi}^B\rangle$, we get the state

$$(-1)^{\boldsymbol{\psi}^A (\boldsymbol{\psi}^B)^T} |\boldsymbol{\psi}^A\rangle_L \otimes |\boldsymbol{\psi}^B\rangle_L. \tag{18}$$

At the same time, if we apply CZ gates to the n pairs of physical qubits, we get

$$\begin{aligned} &\mathrm{CZ}(|\boldsymbol{\psi}^A\rangle_L \otimes |\boldsymbol{\psi}^B\rangle_L) \\ &= \alpha \sum_{\mathbf{y} \in C_2^{\perp}, \mathbf{z} \in C_4^{\perp}} (-1)^{\left(\mathbf{x}^A + \mathbf{y}\right)\left(\mathbf{x}^B + \mathbf{z}\right)^T} |\mathbf{x}^A + \mathbf{y}\rangle \otimes |\mathbf{x}^B + \mathbf{z}\rangle \\ &= \alpha\beta \sum_{\mathbf{y} \in C_2^{\perp}, \mathbf{z} \in C_4^{\perp}} (-1)^{\mathbf{x}^A \mathbf{z}^T + \mathbf{y}\left(\mathbf{x}^B + \mathbf{z}\right)^T} |\mathbf{x}^A + \mathbf{y}\rangle \otimes |\mathbf{x}^B + \mathbf{z}\rangle \end{aligned} \tag{19}$$

where $\alpha = \frac{1}{\sqrt{|C_2^{\perp}||C_4^{\perp}|}}$ and $\beta = (-1)^{\mathbf{x}^A \left(\mathbf{x}^B\right)^T}$. For having a transversal CZ gate, (18) should be equal to (19). Thus, from (18), (8), and (9), we get that (17) must hold. Further

$$\beta = (-1)^{\mathbf{x}^A \left(\mathbf{x}^B\right)^T} = (-1)^{\boldsymbol{\psi}^A \mathbf{A}\mathbf{B}^T \left(\boldsymbol{\psi}^B\right)^T}$$

must be equal to $(-1)^{\boldsymbol{\psi}^A \left(\boldsymbol{\psi}^B\right)^T}$, for all $\boldsymbol{\psi}^A$ and $\boldsymbol{\psi}^B$. This is possible iff $\mathbf{A}\mathbf{B}^T = \mathbf{I}$. ☐

Note that either of the two CSS-codes can be the control or target code. This theorem allows to formulate the following sufficient conditions for CZ-transversality.

Corollary 1. *It is sufficient for codes CSS$(\mathcal{C}_1, \mathcal{C}_2)$ and CSS$(\mathcal{C}_3, \mathcal{C}_4)$ to satisfy the following conditions in order to be CZ-transversal:*

$$\mathcal{C}_1 / \mathcal{C}_2^{\perp} \cong \mathcal{A}_1, \quad \mathcal{C}_3 \subseteq \mathcal{C}_2, \quad \mathbf{A}\mathbf{B}^T = \mathbf{I}, \tag{20}$$

or

$$\mathcal{C}_1 \subseteq \mathcal{C}_4^{\perp}, \quad \mathcal{C}_3 / \mathcal{C}_4^{\perp} \cong \mathcal{B}_1, \quad \mathbf{A}\mathbf{B}^T = \mathbf{I}, \tag{21}$$

where $\mathcal{A}_1 \subset \mathcal{C}_4$ and $\mathcal{B}_1 \subset \mathcal{C}_2$ are group of vectors $\mathbf{c} \in \mathbb{F}_2^n$.

Proof. In order to satisfy (17), it is enough that one of the following conditions holds

- $\mathbf{x}^A \mathbf{z}^T = 0$ and $\mathbf{y}\left(\mathbf{x}^B + \mathbf{z}\right)^T = 0$: this is the case if $\mathcal{C}_1 / \mathcal{C}_2^{\perp} \cong \mathcal{A}_1 \subseteq \mathcal{C}_4$, and $\mathcal{C}_3 \subseteq \mathcal{C}_2$;
- $\mathbf{x}^A \mathbf{z}^T = 1$ and $\mathbf{y}\left(\mathbf{x}^B + \mathbf{z}\right)^T = 1$: this cannot happen since $\mathbf{z}$ belongs to a linear code and therefore it could be $(0, \ldots, 0)$;
- $\left(\mathbf{x}^A + \mathbf{y}\right)\mathbf{z}^T = 0$ and $\mathbf{y}\left(\mathbf{x}^B\right)^T = 0$: this is the case if $\mathcal{C}_1 \subseteq \mathcal{C}_4^{\perp}$, and $\mathcal{C}_3 / \mathcal{C}_4^{\perp} \cong \mathcal{B}_1 \subseteq \mathcal{C}_2$;
- $\left(\mathbf{x}^A + \mathbf{y}\right)\mathbf{z}^T = 1$ and $\mathbf{y}\left(\mathbf{x}^B\right)^T = 1$: this cannot happen since $\mathbf{z}$ belongs to a linear code.

The fact that $\mathbf{A}\mathbf{B}^T = \mathbf{I}$ should be satisfied as well completes the proof. ☐

Below we provide an example of CSS codes that CZ-transversal.

Example 2. *In [3], mirrored CSS codes were proposed, defined by the following generators*

$$\begin{bmatrix} \mathbf{G}_2^{\perp} & \mathbf{0} \\ \mathbf{0} & \mathbf{G}_1^{\perp} \end{bmatrix} \text{ and } \begin{bmatrix} \mathbf{G}_4^{\perp} & \mathbf{0} \\ \mathbf{0} & \mathbf{G}_3^{\perp} \end{bmatrix} = \begin{bmatrix} \mathbf{G}_1^{\perp} & \mathbf{0} \\ \mathbf{0} & \mathbf{G}_2^{\perp} \end{bmatrix}. \tag{22}$$

We further proved that these codes are CZ-transversal. Below we consider an example of such codes and prove that they are

CZ-transversal using Corollary 1. We consider mirrored CSS codes defined by

$$\mathbf{G_1^\perp} = \begin{bmatrix} 1 & 1 & 0 & 0 & 1 & 0 & 0 \\ 1 & 1 & 1 & 0 & 0 & 1 & 0 \\ 1 & 1 & 1 & 0 & 0 & 0 & 1 \end{bmatrix},$$

and

$$\mathbf{G_2^\perp} = \begin{bmatrix} 1 & 1 & 0 & 0 & 0 & 0 & 0 \\ 0 & 1 & 0 & 1 & 1 & 1 & 1 \end{bmatrix}.$$

After simple manipulations we find that

$$\mathbf{G}_4 = \mathbf{G}_1 = \begin{bmatrix} \mathbf{G_2^\perp} \\ \mathbf{A} \end{bmatrix} = \left[\begin{array}{ccccccc} 1 & 1 & 0 & 0 & 0 & 0 & 0 \\ 0 & 1 & 0 & 1 & 1 & 1 & 1 \\ \hdashline 0 & 0 & 1 & 1 & 0 & 1 & 1 \\ 1 & 0 & 1 & 1 & 1 & 0 & 0 \end{array}\right],$$

$$\mathbf{G}_2 = \mathbf{G}_3 = \begin{bmatrix} \mathbf{G_4^\perp} \\ \mathbf{B} \end{bmatrix} = \left[\begin{array}{ccccccc} 0 & 0 & 0 & 0 & 1 & 1 & 0 \\ 0 & 0 & 0 & 0 & 1 & 0 & 1 \\ 1 & 1 & 0 & 0 & 0 & 1 & 0 \\ \hdashline 0 & 1 & 1 & 1 & 0 & 0 & 1 \\ 0 & 1 & 1 & 0 & 0 & 0 & 1 \end{array}\right].$$

We see that $\mathcal{C}_1/\mathcal{C}_2^\perp \subset \mathcal{C}_4$, $\mathcal{C}_3 = \mathcal{C}_2$, and $\mathbf{AB}^T = \mathbf{I}_2$. Thus the conditions (20) are satisfied and the mirrored CSS codes are indeed CZ-transversal.

This examples leads to an alternative proof of CZ-transversality of the mirrored CSS code with generators (22) , based on Corollary 1. The only non-trivial part is to show that matrices $\mathbf{A}$ and $\mathbf{B}$ can be chosen so that $\mathbf{AB}^T = \mathbf{I}$. For this, We first show that $\mathbf{U} = \mathbf{AB}^T$ has full rank.

The (i,j)-th entry of $\mathbf{U}$ is $\mathbf{u}_{i,j} = \mathbf{a}_i \mathbf{b}_j^T$, where $\mathbf{a}_i$ and $\mathbf{b}_j$ are ith and jth row of $\mathbf{A}$ and $\mathbf{B}$, respectively. If $\mathbf{U}$ is not full rank, its columns are dependent; there exists a binary vector $\mathbf{x} = (x_1, x_2, ..., x_n)$ such that $\sum_i x_i \mathbf{a}_i \mathbf{B}^T = \mathbf{0}$. If we define $\mathbf{a}' = \Sigma_i x_i \mathbf{a}_i$, we then have $\mathbf{a}' \in \mathbf{B}^\perp$. According to Example 2, for mirrored CSS codes, code spaces and their duals are related as

$$\mathbf{G_1} = \begin{bmatrix} \mathbf{G_3^\perp} \\ \mathbf{A} \end{bmatrix}, \quad \mathbf{G_3} = \begin{bmatrix} \mathbf{G_1^\perp} \\ \mathbf{B} \end{bmatrix}.$$

For a rank-deficient $\mathbf{U}$ we thus would have $\mathbf{G}_3^\perp = \mathbf{G}_1 \cap \mathbf{B}^\perp$, as $\mathbf{a}'$ is a linear combination of $\mathbf{a}_i \in \mathbf{A} \subset \mathbf{G_1}$. Thus $\mathbf{a}' \in \mathbf{G}_3^\perp$, which means that $\mathbf{G}_1$ is not full rank matrix which is a contradiction. $\mathbf{U}$ has to have full rank.

From the fact that $\mathbf{U}$ has full rank it follows that using Gaussian elimination we can find a $\mathbf{W}$ such that $\mathbf{WU} = \mathbf{WAB}^T = \mathbf{A}'\mathbf{B}^T = \mathbf{I}$.

Depending on the error model, whether it is biased or not, CNOT and CZ transversal codes provide different performance—using CZ transversal codes for realizing non-local CNOTs requires additional Hadamard gates.

V. Simulation Results

In this section, we compare a mirrored structure CZ-transversal code of Example 2, designed for biased errors, with a symmetric CNOT transversal code optimized for depolarizing errors. For both codes we use maximum likelihood decoding defined by biased error probabilities

In the simulation, we only consider two error resources. First, we have two-qubit CNOT gate errors with a depolarizing error model described as follows:

$$\mathcal{N}_{CNOT}(\rho) = (1 - f_{\text{gate}})[II](\rho) + \frac{f_{\text{gate}}}{15} \sum_{i,j=1, ij\neq 1}^{4} [\mathbf{P}_c^i \mathbf{P}_t^j](\rho), \tag{23}$$

where f_{gate} is gate error rate, and $\mathbf{P}_{c/t}^i$ is single-qubit Pauli operator on control/target qubit. Second, we have distance-related transmission errors described as

$$\mathcal{N}(\rho) = (1 - \varepsilon_{de})[I](\rho) + \frac{\varepsilon_{de}}{3}([X] + [Y] + [Z])(\rho), \tag{24}$$

where $\varepsilon_{de} = 1 - e^{-\alpha L}$ denotes the error rate and L is the distance between two neighboring stations, and α shows channel quality. Inserting these into the neighbor-station entanglement swapping procedure, the dominant errors are modeled as (6). We set $\alpha = 0.015$ and assume Bell state purification level $K = 5$. We use logical infidelity as the performance metric which is defined as

$$\epsilon = 1 - \operatorname{Tr}(\boldsymbol{\rho}_i \boldsymbol{\rho}_e), \tag{25}$$

where $\boldsymbol{\rho}_i$ and $\boldsymbol{\rho}_e$ stand for the ideal and practical (erroneous) density matrices after error correction [7].

In Fig. 3, we compare two scenarios. Neighboring stations either use a) two mirrored CSS codes (see Example 2), or b) identical Steane codes. All codes are $[[7,1]]$. The minimum distance of the mirrored structure CSS code is 2, while the Steane code has minimum distance 3. We plot logical infidelity against neighboring station distance and local gate error rate.

When the distance is relatively small, the Steane code has lower logical infidelity. At small distances, depolarizing errors dominate, which the Steane code is better at correcting due to its structure larger minimum distances. In the opposite regime, when the gate error is small and distance-related errors dominate, the mirrored structure CSS code corrects errors more efficiently. This shows that when the biased errors arising from the non-local CNOT gate protocol between stations are relevant, sacrificing minimum distance in order to realize the mirrored structure becomes a viable option.

VI. Conclusion

Motivated by the fact that different quantum systems may suffer from various error models, this paper studies transversality between two different quantum error-correcting codes (QECCs). This generalizes the concept of the transversality in QECCs, different from conventional approach of using the same code in each code blocks. Specifically, by focusing on CSS codes, we identify necessary and sufficient conditions for the transversality of CNOT and CZ gates, which impose less restrictive constraints than having the same CSS codes. Through simulation result, we showed that the performance of CNOT or CZ transversal codes have different optimal regions. A possible future direction is to investigate gates from higher levels of the Clifford hierarchy, such as T-gate to examine the possibility of having universal transversal gate set using

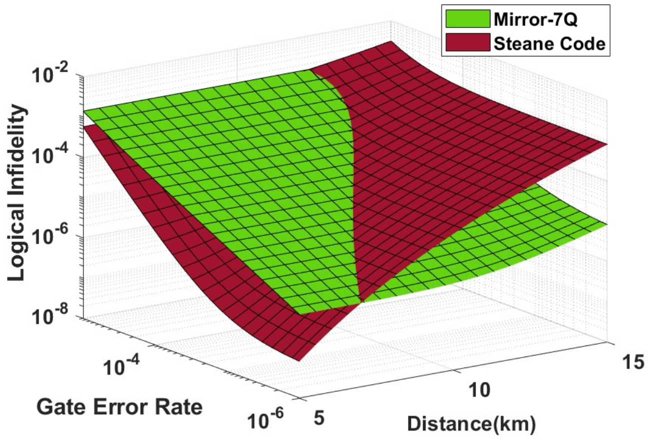

Fig. 3. Comparison of the logical infidelity of the Steane code (CNOT transversal) and mirrored 7-qubit code (CZ transversal) for different gate error rates and distances.

different codes in nearby stations. We believe that the study of transversality is not only limited with the 2nd generation quantum repeaters QRs but could also be applied to construct fault-tolerant quantum computation, e.g., in efficient way to prepare magic state.

ACKNOWLEDGEMENTS

This work was funded in part by the Research Council of Finland (grant 334539) and Nokia Industrial Doctoral School in Quantum Technology.

REFERENCES

[1] D. Gottesman, "An introduction to quantum error correction and fault-tolerant quantum computation," in *Quantum Information Science and Its Contributions to Mathematics, Proc. Symposia in Applied Mathematics 68*, 2009, pp. 13–58.

[2] ——, "Stabilizer codes and quantum error correction," PhD thesis, California Institute of Technology, Pasadena, CA, 1997.

[3] D. Jiao, A. Ashikhmin, M. Bayanifar, and O. Tirkkonen, "Using small dimensional quantum error correction codes for high-performance quantum communication," in *IEEE Global Communications Conference*, 2023, pp. 1387–1392.

[4] P. van Loock, W. Alt, C. Becher, O. Benson, H. Boche, C. Deppe, J. Eschner, S. Höfling, D. Meschede, P. Michler *et al.*, "Extending quantum links: Modules for fiber-and memory-based quantum repeaters," *Advanced quantum technologies*, vol. 3, no. 11, p. 1900141, 2020.

[5] D. Gottesman, "Opportunities and Challenges in Fault-Tolerant Quantum Computation," in *Proc. Solvay Conference on Physics*, May 2022.

[6] X. Zhou, D. W. Leung, and I. L. Chuang, "Methodology for quantum logic gate construction," *Physical Review A*, vol. 62, no. 5, p. 052316, 2000.

[7] M. A. Nielsen and I. L. Chuang, *Quantum Computation and Quantum Information*. Cambridge University Press, 2000.

[8] B. M. Terhal, M. Horodecki, D. W. Leung, and D. P. DiVincenzo, "The entanglement of purification," *Journal of Mathematical Physics*, vol. 43, no. 9, pp. 4286–4298, 2002.

[9] S. Bose, V. Vedral, and P. L. Knight, "Multiparticle generalization of entanglement swapping," *Physical Review A*, vol. 57, no. 2, p. 822, 1998.

[10] S. Muralidharan, L. Li, J. Kim, N. Lütkenhaus, M. D. Lukin, and L. Jiang, "Optimal architectures for long distance quantum communication," *Scientific reports*, vol. 6, no. 1, p. 20463, 2016.

[11] T. J. Yoder, R. Takagi, and I. L. Chuang, "Universal fault-tolerant gates on concatenated stabilizer codes," *Physical Review X*, vol. 6, no. 3, p. 031039, 2016.